Self-Assembled Helices from 2,2′-Biimidazoles

William E. Allen,[b] Christopher J. Fowler,[a] Vincent M. Lynch,[a] and Jonathan L. Sessler*[a]

Abstract: 2,2′-Biimidazoles were synthesized by palladium(0)-catalyzed coupling of 2-iodoimidazoles bearing an alkyl and an ester group at the 4- and 5-positions, respectively. The products were found to be fluorescent and moderately soluble in organic solvents. Three biimidazoles were subjected to single crystal X-ray diffraction analysis. In all three instances, adjacent molecules were found to be bound together in the solid state by pairs of N-H···N hydrogen bonds, forming twisted ribbon-like columns which resemble double helices. The amount of helical twist observed between neighboring biimidazole subunits in these helices varies with the identity of the alkyl and ester groups; in two cases it is approximately 60°, whereas in the third it is about 90°. Mass spectra of six different biimidazoles display ions with masses corresponding to dimers; this indicates that these compounds retain some affinity for each other in the gas phase. The three most soluble biimidazoles also show mass spectrometric peaks ascribable to trimers and tetramers. The solution-phase aggregation tendencies of these latter three compounds were studied by vapor pressure osmometry. In each case, the apparent molecular weight in 1,2-dichloroethane solution is higher than would be expected for free monomers.

Keywords: biimidazoles · helical structures · hydrogen bonds · self-assembly · supramolecular chemistry

Introduction

Biological self-assembly displays a remarkable level of fidelity. All of the information needed to form a particular reproducible structure in vivo, such as a viral capsid, superstructure DNA and RNA, or a specific α-helical polypeptide, is encoded within the sequence and/or structure of the constituent subunits. Construction of synthetic materials by self-assembly[1] rather than by stepwise covalent synthesis is economically desirable, but is hampered by an incomplete understanding of how changes at the single-molecule level influence the properties of the resulting self-assembled material(s).[2] One way to exert some control over the structure of the final assembled product is to exploit hydrogen bonding. H-bonds are directional, and they commonly form only when groups such as NH, OH, and C=O are present.[3] Thus, the use of building blocks with carefully positioned complementary hydrogen-bonding functionality can increase the odds of producing ensembles where the individual subunits are arranged in an expected way. This strategy has been used to produce a variety of architectures, including pseudospheres,[4] artificial protein β-sheets,[5] duplexes with unnatural backbones,[6] molecular "zippers",[7] catenanes,[8] dendrimers,[9] and grids.[10]

A structure which has been particularly inspiring to synthetic chemists is the helix, as it occurs throughout Nature. To date, a number of different approaches to the production of artificial helical structures have been pursued. Molecules like helicenes, Lehn's polyheterocyclic strands,[11] and Moore's *m*-phenylacetylene oligomers[12] define an "all-covalent" paradigm, in which the subunits are compelled to adopt helical shapes in order to reduce steric crowding imposed by their covalent frameworks. Interactions between transition metal ions and oligopyridine ligands have also been used to prepare single-, double-, and multiple-helical arrays. This "metal-template" approach, developed by the research groups of Lehn,[13] Constable,[14] Newkome,[15] Sauvage,[16] and many others,[17] takes advantage of the propensity of metal ions such as Cu^{I} to assume predictable coordination geometries. The molecular information required for helix

[a] Prof. Dr. J. L. Sessler, Dr. C. J. Fowler, Dr. V. M. Lynch
Department of Chemistry and Biochemistry
Institute for Cellular and Molecular Biology
The University of Texas at Austin, Austin, TX 78712-1167 (USA)
Fax: (+1) 512-471-7550
E-mail: sessler@mail.utexas.edu

[b] Prof. W. E. Allen
Department of Chemistry, East Carolina University
Greenville, NC 27858-4353 (USA)

Supporting information for this article is available on the WWW under http://www.wiley-vch.de/home/chemistry/ or from the author. Details for the syntheses of **14**, **15**, and **16**; complete X-ray experimental, figures showing atomic numbering schemes, tables of bond lengths and angles, and tables of positional and thermal parameters for **12**, **11**, and **9**.

  0947-6539/01/0703-0721 $ 17.50+.50/0

formation is thus encoded in the various metal–ligand dative bonds. This same sort of "information" has also been used to generate helical motifs by attaching polypeptide chains to metal–ligand complexes.[1a, c]

While metal-coordinated systems have been studied in great detail by numerous researchers, the appealing alternative of using hydrogen bonding or base-pair-like interactions to stabilize synthetic helical arrays has also received attention.[18] In early seminal work, Hamilton et al. generated a self-assembling double helical structure by exploiting amide–carboxylic acid pairing.[18a] Lehn's group examined the behavior of mixtures of tartaric acid-based derivatives, one containing donor–acceptor–donor atoms and the other an acceptor–donor–acceptor array.[18b] These molecules interacted via complementary uracil/2,6-diamidopyridine base pairs to form helical structures. Other hydrogen bonding and base-pairing interactions have been used to form related architectures in more recent years.[18c–k] For instance, interactions between tartaric acid derivatives and bipyridyls have been shown by Singh et al. to form supramolecular assemblies under conditions of thermal induction in the solid state.[18c] Reinhoudt and co-workers used enantiomerically pure calix[4]arene dimelamines and 5,5-diethylbarbituric acid to form chiral hydrogen-bonded structures that display helical one-handedness.[18d] Hydrogen bonding between hydroxyl groups has been exploited to create enantiospecific formations of helical tubands[18e] and a four leaf clover motif.[18f] Hydroxyl–pyridine interactions were used separately by Mazik et al. to generate a multi-component array with an inner channel of diameter 14 Å.[18g] Hydrogen bonding and π-stacking interactions have been used in tandem to stabilize both single- and triple-helical structures.[18h,i]

While elegant, each of these approaches is characterized by its own set of strengths and weaknesses, which means that the search for new molecules capable of undergoing hydrogen bond mediated self-assembly remains cogent. In this paper we demonstrate that derivatized 2,2′-biimidazoles can serve as precursors to solid-state hydrogen-bonded helices. 2,2′-Biimidazole **1** was chosen as the functional nucleus of our supramolecular monomers, because it is capable of simultaneously serving as both a hydrogen-bond donor and acceptor, and it is known to spontaneously form polymeric chains in the solid state.[19] While such chains of **1** are flat, sterically encumbered biimidazoles (**9**, **11**, and **12**, see Scheme 1), the synthesis of which is reported here, are found to self-assemble into spiral columns in the crystal. These columns bear a striking, albeit "reversed", resemblance to helical duplex DNA.

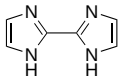

1

Results and Discussion

In order to serve as building blocks for self-assembled structures, 2,2′-biimidazoles need to be rendered soluble in organic solvents since this choice of media will enhance their propensity to form intermolecular N-H···N bonds. This requirement for solubility compels, in turn, the development of a facile derivatization strategy that will not block either the NH hydrogen bond donor or N lone pair acceptor sites. Such a strategy does not currently exist.

Previously, it was found that the NH groups of **1** could be protected using [2-(trimethylsilyl)ethoxy]methyl[20] (SEM) groups. This affords an organic-soluble material which can be further functionalized by halogenation[21] or lithiation.[22] Unfortunately, the introduction of SEM, or other NH protecting groups, eliminates the potential for hydorgen bonding. A more attractive approach to attaining organic-soluble 2,2′-biimidazoles involves placing solubilizing substituents at the 4-, 4′-, 5-, and 5′-positions. Such biimidazoles have been produced by classical ring-closing reactions involving diamides.[23, 24] They can also be obtained by subjecting unsubstituted **1** to harsh reaction conditions.[25, 26] In either case, it is important to appreciate that such biimidazoles are known only where the four substituents are identical (e.g., tetramethyl,[23] tetraphenyl,[24] tetrabromo,[25] and tetranitro[26]). These derivatives are also relatively insoluble in organic media.

Synthesis: Our approach to generating solubilized 2,2′-biimidazoles with free hydrogen-bonding groups was predicated on the use of a transition metal mediated homocoupling strategy (Scheme 1). Specifically, starting with imidazoles **2**, **3**, and **4**, halogenation at the unblocked 2-position provided the precursors needed for coupling (i.e., **5**–**7**).

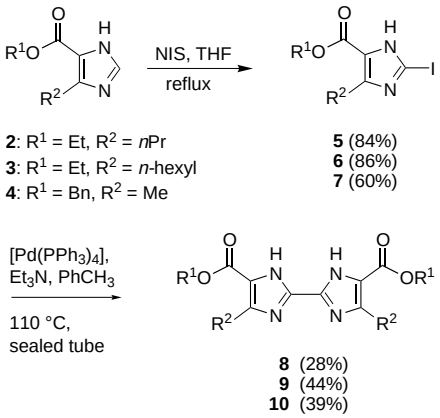

Scheme 1. Palladium(0)-catalyzed synthesis of substituted biimidazoles.

The starting materials **2**–**4** were readily obtained. Ethyl 4-propyl-5-imidazolecarboxylate (**2**), a known compound,[27] was prepared by chlorinating ethyl butyrylacetate with SO_2Cl_2, and cyclizing the resulting product in formamide/water at reflux as previously described.[28] Following a similar chlorination/cyclization procedure, hexyl-substituted imidazole **3** was synthesized from ethyl 3-oxononanoate.[29] Imidazole **4** was prepared by base-catalyzed transesterification of commercially available ethyl 4-methyl-5-imidazolecarboxylate in benzyl alcohol.

Attempts to iodinate compound **2** in the 2-position using molecular iodine[30] (1 equiv I_2, $CHCl_3$/aq NaOH) failed to provide any halogenated product; in contrast, treatment with *N*-iodosuccinimide (NIS) in tetrahydrofuran (THF) while

0947-6539/01/0703-0722 $ 17.50+.50/0 *Chem. Eur. J.* **2001**, *7*, No. 3

heating at reflux afforded the desired iodide **5** in 84% yield. Other halogenated derivatives of imidazole **2** could be prepared using Br_2/NaOAc/HOAc, or by protecting the NH groups of **2** with the SEM group prior to iodination.[31] However, isolation of the products required column chromatography. So, the requisite coupling precursors (i.e., **5**, **6**, and **7**) were most conveniently prepared by iodination of **2**–**4** with NIS.

Unlike the coupling of 4-iodoimidazoles,[30] which fails if the imidazole-NH groups are not protected, 2-iodoimidazoles **5**–**7** were successfully coupled using catalytic amounts of tetrakis(triphenylphosphine)palladium(0). Sealed-tube reaction of iodide **5** with $[Pd(PPh_3)_4]$ (4 mol%) and triethylamine (2 equiv) under argon while heating in toluene at 110°C for 48 h produced the symmetrical biimidazole **8** in 28% yield, after collecting the precipitated product by filtration and purifying it by recrystallization from methanol. Applying the same reaction conditions, biimidazoles **9** and **10** were synthesized in yields of 44% and 39%, respectively. Heterocoupling of iodides **6** and **7** gave a mixture of products from which the unsymmetrical biimidazole **11** could be isolated in 15% yield after column chromatography on silica gel using hexanes/EtOAc/CH_2Cl_2 (6:4:1 *v*/*v*/*v*) as eluents (Scheme 2). Increasing

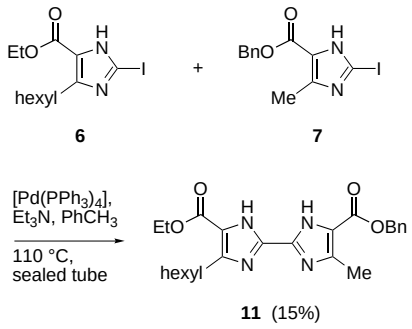

Scheme 2. Palladium(0)-catalyzed synthesis of asymmetric biimidazole **11**.

the temperature of the coupling reactions to 120–130°C, or using DMF as the reaction solvent,[30] did not improve the yields. No coupling was observed in the absence of triethylamine. Other possible transition metal-assisted routes to biimidazoles were explored, and were found to be inferior to the present procedure. For instance, attempted Ullmann coupling of **5** (5 equiv Cu^0), toluene or DMF, 110°C) did not produce biimidazole product **8**[32] and gave dehalogenated material instead. Using nickel(0) as the coupling promoter[33] (0.5 equiv $Ni(COD)_2$, toluene, rt, irradiation with 500 W lamp) provided the desired product **8**, but only in low yield (12% after column chromatography on silica gel using EtOAc as the eluent).

Two additional biimidazoles were synthesized from **8**. Transesterification using methanol and sodium hydroxide gave the dimethyl diester **12** in 63% yield, while the tetraalkyl derivative **13** was prepared in 92% yield by exhaustive reduction of the ester groups of **8** with lithium aluminum hydride in THF (Scheme 3).

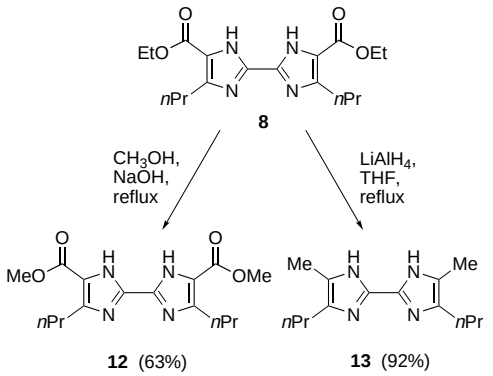

Scheme 3. Transesterification and reduction of biimidazole **8**.

Spectroscopy: The electronic absorption spectra of diesters **8**–**12**, recorded in dichloromethane, are all characterized by an absorbance maximum near 295 nm. The fluorescence maximum for these (aerated) samples occurs around 350 nm. The fluorescence emission appears intensely violet-blue to the naked eye. Only **13**, which lacks carboxylate groups, shows somewhat different spectroscopic behavior. It is characterized by an absorbance band at 298 nm and an emission band at 373 nm.

Solid-state helices: The modest organic solubility of the first biimidazole we prepared, **8**, provided a first hint that this class of tetrasubstituted biimidazoles might self-assemble into hydrogen-bonded networks in the solid state, as desired. While repeated attempts to obtain crystals of **8** suitable for X-ray diffraction analysis failed, high-quality single crystals of the homologous biimidazole **12** could be obtained by allowing a methanol solution to undergo slow evaporation. A representative view of molecule **12**, doubly hydrogen-bonded with the two nearest neighbors, is shown in Figure 1. The two propyl substituents are found at opposite corners of the biimidazole, in an *anti* relationship to one another. The imidazole N*H* atoms were located and refined, and found to reside on the nitrogen atoms next to the alkyl groups. Intramolecular $N\text{-}H\cdots O_{ester}$ hydrogen bonding is not ob-

Table 1. Crystal data for $(C_{16}H_{22}N_4O_4)_3\cdot(CH_3OH)_{0.5}$ (**12**), $C_{24}H_{30}N_4O_4$ (**11**), and $(C_{24}H_{38}N_4O_4)_4\cdot(CH_3OH)_{0.5}$ (**9**).

	12	**11**	**9**
formula	$C_{48.5}H_{68}N_{12}O_{12.5}$	$C_{24}H_{30}N_4O_4$	$C_{96.5}H_{154}N_{16}O_{16.5}$
M_w	1019.15	438.52	1802.36
crystal system	monoclinic	triclinic	monoclinic
space group	*C*2/*c*	*P*	$P2_1/n$
color	colorless	colorless	colorless
a [Å]	21.589(2)	16.0220(5)	24.218(3)
b [Å]	28.437(3)	21.838(1)	17.867(2)
c [Å]	19.203(2)	22.585(1)	24.921(3)
α [°]	90.0	68.716(2)	90.0
β [°]	112.57(1)	71.315(3)	96.79(1)
γ [°]	90.0	80.287(3)	90.0
V [Å^3]	10886(2)	6962.8(5)	10708(2)
Z	8	12	4
T [K]	193(2)	203(2)	188(2)
R	0.0739	0.0962	0.124
R_W	0.1315	0.120	0.217
GOF	1.521	1.228	1.134

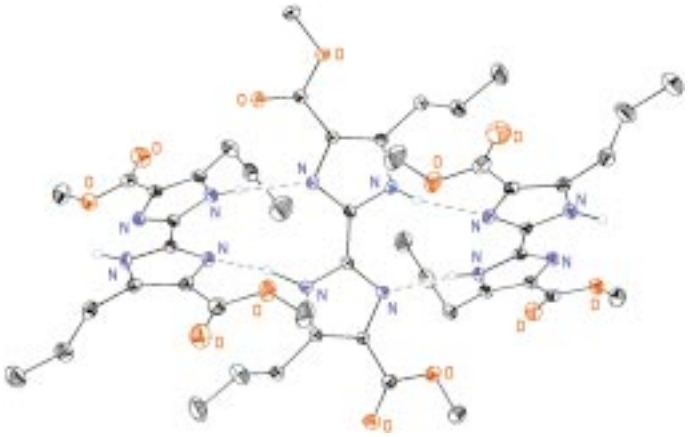

Figure 1. Molecular structure of biimidazole **12** showing hydrogen bonding to the nearest two neighboring molecules. Thermal ellipsoids are scaled to the 50% probability level. Hydrogen atoms on the imidazole nitrogens are drawn arbitrarily small. Oxygen and nitrogen atoms are labeled, and are colored red and blue, respectively.

served in the crystal, even though such hydrogen bonding would produce five-membered rings. The central C–C bond lengths (C2–C6) found for the three crystallographically independent molecules of **12** are 1.448(5) Å, 1.445(5) Å, and 1.439(5) Å. These values are similar to those observed in **1** (1.423(8) Å) and in 4,4′,5,5′-tetranitro-2,2′-biimidazole (as dihydrate, 1.441(1) Å; as diammonium salt, 1.451(1) Å).[26] Unlike these latter structures, however, in which the imidazole rings are coplanar, the rings in each of the three unique molecules of **12** are rotated by 9.4(0.4)°, 24.5(0.1)°, and 18.3(0.2)° about their respective central C–C bonds.

The hydrogen bonding between molecules of **12** gives rise to infinitely long columns which propagate parallel to the *b* axis of the crystal. Measured center-to-center, the separation between columns is 10.8 Å and 9.6 Å in the *a* and *c* directions, respectively. A portion of one of the columns is shown in Figure 2a. The intermolecular N···N distances between adjacent biimidazoles in a column range from 2.878(4) Å to 3.085(5) Å, indicative of strong N-H···N hydrogen bonding. The two separate hydrogen-bonding paths, shown as dashed lines in Figure 2a, twist about a mutual axis in a double helical fashion. The amount of twist on moving from one biimidazole to the next, given by the dihedral angle between the C2–C6 bonds of adjacent molecules, averages 60°. The pitch per one complete turn of the helix is 29.4 Å, corresponding to a rise of 4.9 Å per biimidazole. While Figure 2a shows only a right-handed helix, the bulk crystals of **12** are not chiral—any right-handed twist in one column is offset by an equivalent left-handed twist in an adjacent column.

The "mixed" biimidazole **11**, with four different groups at the 4-, 4′-, 5-, and 5′-positions, was also subjected to X-ray diffraction analysis. The resulting structure revealed six unique (albeit very similar) molecules (of **11**) in the crystal. All six display an *anti* relationship between the methyl and hexyl groups, and the amount of tilt between the imidazole rings of each biimidazole was found to be 18.6°, 16.7°, 17.1°, 16.9°, 21.7°, and 23.6°, respectively. Biimidazole **11** (Figure 2c) self-assembles into twisted columns with structural properties resembling those of **12**. The hydrogen-bonding distances

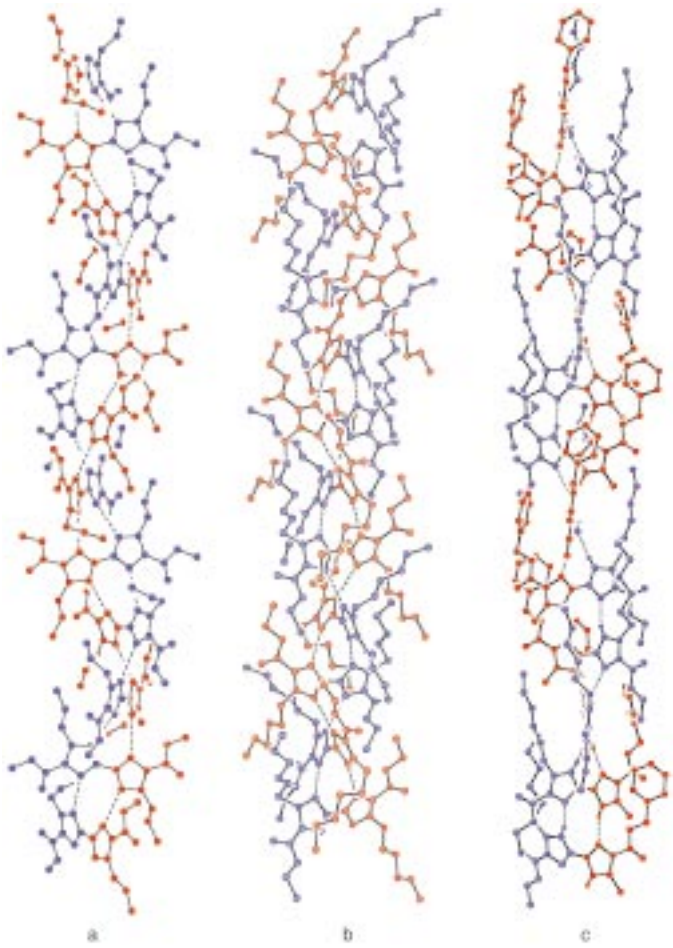

Figure 2. Right-handed helices formed from **12** a), **9** b), and **11** c). Each ribbon contains 12 biimidazole subunits that are divided at the 2,2′ bond by red and blue coloring in order to clarify the helical progression of the column. Hydrogen bonds are shown as dashed lines. Columns a) and c) complete two full rotations while b) completes three.

between neighboring biimidazoles within a column range from 2.885(4) Å to 3.048(5) Å, and like **12**, the dihedral angle between the central C–C bonds of adjacent molecules averages 60°. The pitch of the helix for **11** (29.2 Å) is nearly identical to that of **12**. From the perspective of any single helix, there will be six neighboring helices; because of symmetry considerations, there are three unique column-to-column contacts. Measured center-to-center, these distances are 11.6 Å, 11.8 Å, and 11.8 Å. Helices formed from **11** display an additional level of organization which is not possible for **12**. Using a "twisted ladder" analogy, one of the "uprights" of the ladder consists only of hexyl group/ethyl ester-substituted imidazoles, while the other "upright" consists of only methyl group/benzyl ester-type imidazoles.

X-ray diffraction analysis of the dihexyl-substituted biimidazole **9** was also carried out. It revealed the expected *anti* configuration of alkyl groups. In this case, however, the two imidazole rings of **9** display a pronounced tilt relative to one another which averages 42.4°. As in **12** and **11**, molecules of **9** self-associate in the solid state to produce double-helical columns which run along the crystallographic *b* axis, although the center-to-center distances between the columns are

0947-6539/01/0703-0724 $ 17.50+.50/0 *Chem. Eur. J.* **2001**, *7*, No. 3

slightly larger for **9** (12.1 Å and 12.4 Å in the *a* and *c* directions, respectively). Figure 2b shows part of one of the columns. The quality of the data did not allow the N*H* protons to be located, but the short intermolecular N···N distances (averaging 2.8 Å) are consistent with hydrogen bonding occurring between adjacent members of a helix. In contrast to **12** and **11**, helices formed from **9** display a 90° twist from molecule to molecule, and a pitch per full turn of only 18 Å. Biimidazole **9** thus displays the greatest degree of intramolecular imidazole–imidazole rotation and the most pronounced helical twist between molecules.

While double helical in aspect, the supramolecular structures formed from **9**, **11**, and **12** are not strictly DNA-like. Rather, they can be viewed as being as "reversed" or "inverted." The backbone of DNA is constructed from covalent bonds, while its two individual strands are bound together through hydrogen bonding between base pairs. In the case of the present helices, each biimidazole subunit can be considered as representing a covalently linked "base pair" (i.e., a pair of 2,2′-linked imidazoles). By contrast, the "backbone" of the helices are formed by hydrogen-bonding interactions, as opposed to phosphodiester linkages.

Figure 3, drawn to scale for one full rotation in each helix, provides a graphical comparison between **12** and B-form DNA. Among other things, Figure 3 helps highlight how the various dimensional features of these two helical structures are different; these comparisons are summarized in Table 2. Along the helix axes, DNA is clearly more compressed. In the case of **12**, only six biimidazoles are required to complete one 360° rotation of the helix, while a full turn of B-DNA contains ten base pairs. However, the vertical pitch (i.e., the distance covered in one full rotation) is similar in both structures, measuring 29.4 Å for biimidazole **12** versus 34 Å for B-form DNA. The greater rise per "base pair" in the case of **12** results from the fact that in order to remain hydrogen bonded, adjacent biimidazoles must approach each other in an approximately edge-on manner, and cannot closely stack face-to-face as do the base pairs of DNA. While hydrogen bonding serves a different supramolecular function in the natural and synthetic structures, the average hydrogen-bond distances for both types of helices were found to be virtually identical, namely 2.9 Å. This latter congruence serves to underscore how a given type of intermolecular interaction, hydrogen bonding in this case, can be expressed in terms of a wide range of supramolecular structures.

Table 2. Dimensional analysis of the helical ribbon formed from biimidazole **12** and B-DNA, as represented in Figure 3.

	Double helix	
	12	B-DNA
"base pairs" per 360° turn	6	10
pitch	29.4 Å	34 Å
vertical rise per "base pair"	4.9 Å	3.4 Å
helix diameter	10 Å	20 Å
hydrogen-bond distance	2.9 Å	2.9 Å

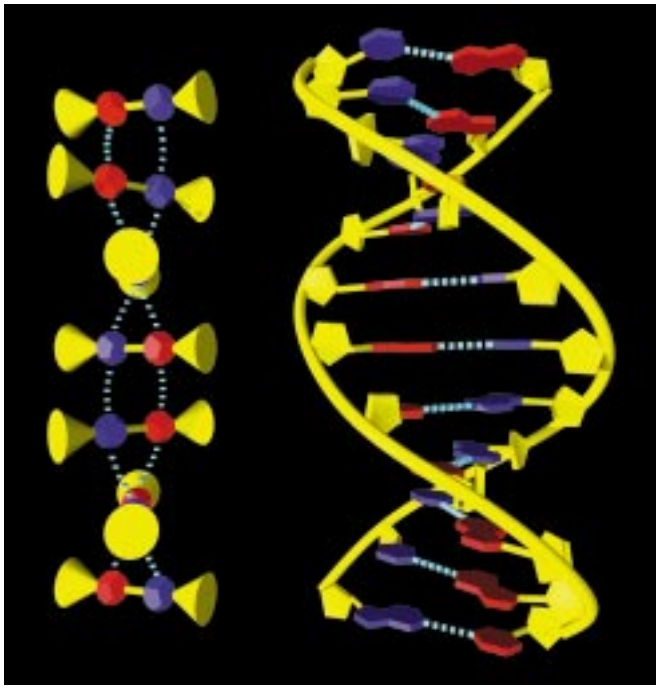

Figure 3. Schematic representations of biimidazole **12** and B-DNA, drawn to scale. See Table 2 for dimensional analysis.

Self-association in the gas and liquid phases: In order to determine whether self-associated biimidazole oligomers persist in the gas phase, saturated dichloromethane solutions of **8**–**13** were analyzed using mass spectrometry (MS) in chemical ionization (CI) and fast-atom bombardment (FAB) modes. As shown in Table 3, an ion with $m/z = [2M]^+$, presumably arising from a non-covalent dimer, is observed for all six samples tested in both ionization modes. The monomeric form of the biimidazoles is dominant in CI mode; this gives rise to the base peak in each spectrum, but peaks corresponding to trimers and even tetramers are nevertheless observed for the three most soluble biimidazoles **9**–**11**. When FAB ionization is used, the extent of observed oligomerization is generally lower, except in the case of **9**. Under these analysis conditions, the peak corresponding to a dimer of **9** ($m/z = 893$) is approximately fourteen times more intense than that for the monomer (Figure 4). In additional

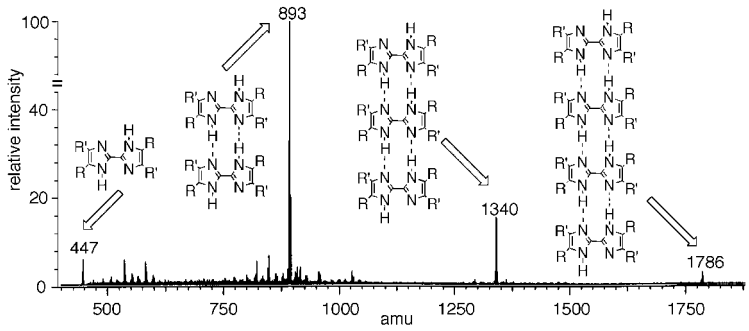

Figure 4. Mass spectrum of a dichloromethane solution of **9**, analyzed in FAB ionization mode.

MS experiments, not shown in Table 3, methanol solutions of **9** and **10** were analyzed in CI mode. This was done in order to assess the influence of solvent on the gas-phase aggregation properties of these representative species. For **9**, the relative intensity of the dimer ion fell from 39 in dichloromethane to 7 in methanol. For methanol solutions of **10**, no higher-order peaks were observed at all. Such findings are consistent with the premise that intermolecular hydrogen-bonding interactions are responsible for ensemble formation in the fluid phase as in the solid state.

Table 3. Mass spectrometric data for 2,2′-biimidazoles.[a]

biimidazole tetramer	ionization mode	observed peaks [m/z (%)] monomer	dimer	trimer
8	CI	363 (100)	725 (1)	
9	CI	447 (100)	894 (39)	1340 (11)	1786 (1)
10	CI	431 (100)	861 (8)	1291 (4)	1721 (1)
11	CI	439 (100)	878 (21)	1316 (12)	1755 (1)
12	CI	335 (100)	669 (28)	1003 (2)	
13	CI	247 (100)	493 (12)	732 (2)	
8	FAB	363 (62)	725 (1)	
9	FAB	447 (7)	893 (100)	1340 (16)	1786 (3)
10	FAB	431 (85)	861 (6)	1291 (1)	
11	FAB	439 (100)	877 (18)	1316 (2)	
12	FAB	335 (100)	669 (2)		
13	FAB	247 (100)	493 (2)		

[a] Chemical ionization (CI) and fast-atom bombardment (FAB) measurements run dichloromethane solutions at the UT-Austin, Department of Chemistry and Biochemistry MS Facility.

In accord with the MS results, vapor pressure osmometry (VPO) measurements provided evidence consistent with the contention that biimidazoles **9**–**11** self-associate in solution (Table 4). The average molecular weights observed for solutions of **9** and **10** in 1,2-dichloroethane are approximately those expected for self-assembled trimers (**9**: $M_{found}/M_{calcd} = 2.8$; **10**: $M_{found}/M_{calcd} = 3.3$). By contrast, the average molecular weight recorded for solutions of the unsymmetrical biimidazole **11** is that expected for a dimer ($M_{found}/M_{calcd} = 1.9$). Biimidazole **8** proved too insoluble in dichloroethane to allow for reliable VPO analysis.

Table 4. Solution-phase molecular weights for 2,2′-biimidazoles in 1,2-dichloroethane as measured by vapor pressure osmometry (VPO).

biimidazole	Calcd monomer MW [g mol^{-1}]	Exptl MW [g mol^{-1}]
9	446	1241
10	430	1399
11	438	827

In conclusion, compounds **9**, **11**, and **12** define a new class of supramolecular monomers which self-associate through multiple hydrogen bonds to produce helices, and thus mimic some characteristics of naturally-occurring macromolecules.[34] They help to illustrate the range of architectures that may be obtained through the judicious use of multifunctional monomers, in this case ones capable of serving concurrently as both hydrogen-bond donors and acceptors. They also highlight in a dramatic way how simple changes in subunit structure can effect the way in which, or even whether, a helix is formed. In the solid state, for example, simple 2,2′-biimidazole **1** forms one-dimensional chains in which all of the imidazole rings are coplanar.[19] By contrast, in helices formed from **9**, **11**, and **12**, steric congestion necessitates that the individual imidazoles of each molecule deviate from coplanarity in order for short intermolecular hydrogen bonds to be maintained. Furthermore, the side chains of **9**, **11**, and **12** not only induce helicity in the columns; these substituents are themselves found to pack in a helical fashion. These ancillary helical features are most noticeable in the case of mixed biimidazole **11.** Here, as illustrated in Figure 5, the benzyl ester and hexyl chains are seen to wrap individually in a right-handed fashion around the helical core. Presumably, the incorporation of other groups on the single-biimidazole periphery may allow for the generation of helices with as yet unobserved geometries.

Figure 5. Space-filled representation of the solid-state structure of biimidazole **11** (Figure 2c), showing how the benzyl ester (red) and hexyl (blue) side chains wrap around the biimidazole core in a helical fashion.

Experimental Section

Ethyl 4-propyl-5-imidazolecarboxylate[28] and ethyl 3-oxononanoate[29] were prepared according to the published procedures. Tetrahydrofuran and toluene were dried by distillation from Na/benzophenone and Na, respectively. All other solvents and reagents were obtained from commercial sources and used as received. Proton and ^{13}C NMR spectra were recorded on a General Electric QE-300 instrument; chemical shifts are reported in ppm relative to internal TMS (for samples in $CDCl_3$) or relative to protons/carbon atoms in the deuterated solvent used. Electronic absorption spectra were acquired on a Beckman DU 640B spectrophotometer. Fluorescence measurements were performed by exciting 5×10^{-5} M dichloromethane solutions at 295 nm, using a Perkin–Elmer LS-5 spectrophotometer. Low- and high-resolution mass spectra were obtained upon dichloromethane solutions at the UT-Austin Department of Chemistry and Biochemistry MS Facility. Vapor pressure osmometry (VPO) was performed by Galbraith Laboratories, Inc., Knoxville, TN. VPO measurements were made at 27 °C upon samples which were $2.5-7.0 \times 10^{-2}$ M in 1,2-dichloroethane, using benzil as the instrument standard. Elemental Analyses were performed by Atlantic Microlab, Inc., Norcross, GA.

Ethyl 4-hexyl-5-imidazolecarboxylate (3): Ethyl 3-oxononanoate (40.1 g, 0.200 mol) was dissolved in chloroform (40 mL) in a 250 mL three-necked flask. A thermometer was immersed in the stirring solution, and dropwise addition of sulfuryl chloride (27.0 g, 0.200 mol) was begun. The rate of addition was controlled such that the temperature of the reaction did not rise above 35 °C. During the course of this addition, the mixture became cloudy, and gas evolution was observed. Once the addition was completed, the mixture was stirred for an additional 30 min. At this juncture, a condenser was fitted to the flask and the contents heated to reflux. After 2 h, the resulting colorless mixture was allowed to cool, washed sequentially with water and saturated aqueous potassium bicarbonate, and dried over Na_2SO_4. Filtration and evaporation of the solvent left a colorless, mobile liquid, which was purified by short-path vacuum distillation. The product so obtained, ethyl 2-chloro-3-oxononanoate (40.3 g, 86%), was

0947-6539/01/0703-0726 $ 17.50+.50/0 *Chem. Eur. J.* **2001**, *7*, No. 3

used directly without further purification. Specifically, ethyl 2-chloro-3-oxononanoate (32.2 g, 0.137 mol), formamide (61.7 g, 1.37 mol), and water (4.93 g, 0.274 mol) were combined in a 250 mL round-bottomed flask containing a stir bar. The mixture was heated at reflux for 3 h, during which time it became dark red. Upon standing at room temperature overnight, a dark red oil separated out, floated to the top of the mixture, and solidified. This solid was collected by vacuum filtration, washed with water, and allowed to dry in the vacuum-induced stream of air for 15 min. A clean filter flask was exchanged for the first one, and dichloromethane was poured onto the filter cake. Most of the material dissolved. The filtrate was dried over Na_2SO_4, filtered, and taken to dryness on a rotary evaporator. This yielded a red-brown oil which partially crystallized upon standing. This crude product was purified by dissolving it in the minimum amount of 2-propanol, and chilling the flask in a freezer overnight to yield light tan crystals (5.20 g, 17%). An additional amount of product **3** (3.99 g, 13%) was obtained by evaporating the mother liquor and subjecting the viscous oil to flash column chromatography over silica gel using EtOAc as the eluent. M.p. 139–140 °C; t_R (EtOAc): 0.38; ^{1}H NMR ($CDCl_3$): $\delta = 0.86$ (t, 3H, $CH_2CH_2CH_2CH_2CH_2CH_3$), 1.1–1.4 (m, 6H, $CH_2CH_2CH_2CH_2CH_2CH_3$), 1.36 (t, 3H, OCH_2CH_3), 1.67 (m, 2H, $CH_2CH_2CH_2CH_2CH_2CH_3$), 2.96 (t, 2H, $CH_2CH_2CH_2CH_2CH_2CH_3$), 4.36 (q, 2H, OCH_2CH_3), 7.72 (s, 1H, imid. C_2H); ^{13}C NMR ($CDCl_3$): $\delta = 18.0$, 18.3, 26.0, 29.5, 32.0, 32.4, 34.4, 61.5, 83.9, 125.3, 142.8, 156.1; LRMS (CI+): m/z (%): 225 (100) $[M+H]^+$; HRMS (CI+): calcd for $C_{12}H_{21}N_2O_2$ 225.1603; found 225.1611; elemental analysis calcd (%) for $C_{12}H_{20}N_2O_2$: C 64.26, H 8.99, N 12.49; found: C 64.17, H 8.93, N 12.42.

Benzyl 4-methyl-5-imidazolecarboxylate (4): A 500 mL round-bottomed flask containing a stir bar was charged with ethyl 4-methyl-5-imidazolecarboxylate (15.4 g, 0.10 mol), a single pellet of solid NaOH (≈0.2 g), and benzyl alcohol (205 mL). A short-path distillation apparatus was fitted to the flask, and the contents were then heated to 110 °C. After 24 h, the temperature of the reaction mixture was raised to 140 °C, and the system was placed under vacuum (4 mm Hg). After approximately 125 mL benzyl alcohol had been distilled off, the crude product started to precipitate in the reaction flask. The vacuum was removed, and the flask was allowed to cool undisturbed to rt. The crude product was collected by filtration and washed with small portions of ice-cold absolute ethanol until the washings were colorless. Recrystallization from absolute ethanol afforded **4** as off-white plates (15.2 g, 70%). M.p. 202–203 °C; ^{1}H NMR (CD_3OD): $\delta = 2.46$ (s, 3H, CH_3), 5.30 (s, 2H, OCH_2Ph), 7.25–7.45 (m, 5H, Ar*H*), 7.59, (s, 1H, imid. C_2H); ^{13}C NMR ([D$_6$]DMSO): $\delta = 11.0$, 64.8, 127.9, 128.4, 134.7, 136.6, 163.0; LRMS (CI+): m/z (%): 217 (100) $[M+H]^+$; HRMS (CI+): calcd for $C_{12}H_{13}N_2O_2$ 217.0977; found 217.0970; elemental analysis calcd (%) for $C_{12}H_{12}N_2O_2$: C 66.65, H 5.59, N 12.95; found: C 66.73, H 5.62, N 12.89.

Ethyl 2-iodo-4-propyl-5-imidazolecarboxylate (5): An oven-dried 250 mL round-bottomed flask containing a stir bar was charged with dry THF (100 mL) and ethyl 4-propyl-5-imidazolecarboxylate (**2**, 9.11 g, 50.0 mmol). After stirring was commenced, the resulting suspension was treated with *N*-iodosuccinimide (95%, 11.8 g, 50.0 mmol) all at once. The flask was then wrapped in foil to exclude light, and the contents heated to reflux under Ar. After 24 h, the reaction was allowed to cool to room temperature, and saturated aqueous $Na_2S_2O_3$ was added dropwise until the iodine color was discharged. The mixture was diluted with equal volumes of EtOAc and water, and the layers were separated. The organic phase was washed with brine, dried over $MgSO_4$, filtered, and evaporated to dryness to yield a yellow solid. Recrystallization from EtOAc afforded the desired product **5** (12.9 g, 84%) as white needles. M.p. 194–195 °C; ^{1}H NMR ($CDCl_3$): $\delta =$ 0.91 (t, 3H, $CH_2CH_2CH_3$), 1.20 (t, 3H, OCH_2CH_3), 1.68 (m, 2H, $CH_2CH_2CH_3$), 2.98 (t, 2H, $CH_2CH_2CH_3$), 4.26 (q, 2H, OCH_2CH_3); ^{13}C NMR ($CDCl_3$): $\delta = 13.8$, 14.2, 22.6, 28.1, 60.4, 84.3, 128.9, 147.0, 161.7; LRMS (CI+): m/z (%): 309 (100) $[M+H]^+$; HRMS (CI+): calcd for $C_9H_{14}N_2O_2I$ 309.0100; found 309.0093; elemental analysis calcd (%) for $C_9H_{13}N_2O_2I$: C 35.08, H 4.25, N 9.09; found: C 35.19, H 4.28, N 9.08.

Ethyl 4-hexyl-2-iodo-5-imidazolecarboxylate (6): Following the method described for **5** above, **3** (0.97 g, 4.3 mmol) in dry THF (20 mL) was iodinated with NIS. Recrystallization from EtOAc afforded the desired iodide **6** (1.30 g, 86%) as white needles. M.p. 116–117 °C; ^{1}H NMR ($CDCl_3$): $\delta = 0.83$ (t, 3H, $CH_2CH_2CH_2CH_2CH_2CH_3$), 1.2–1.5 (m, 6H, $CH_2CH_2CH_2CH_2CH_2CH_3$), 1.27 (t, 3H, OCH_2CH_3), 1.65 (m, 2H, $CH_2CH_2CH_2CH_2CH_2CH_3$), 2.97 (t, 2H, $CH_2CH_2CH_2CH_2CH_2CH_3$), 4.30 (q, 2H, OCH_2CH_3); ^{13}C NMR ($CDCl_3$): $\delta = 18.0$, 18.3, 26.0, 29.5, 32.0, 32.4, 34.4, 61.5, 83.9, 125.3, 142.8, 156.1; LRMS (FAB+): m/z (%): 351 (100) $[M+H]^+$; HRMS (FAB+): calcd for $C_{12}H_{20}N_2O_2I$ 351.0570; found 351.0568; elemental analysis calcd (%) for $C_{12}H_{19}N_2O_2I$: C 41.16, H 5.47, N 8.00; found: C 41.29, H 5.49, N 7.87.

Benzyl 2-iodo-4-methyl-5-imidazolecarboxylate (7): Following the method described for **5** above, **4** (2.95 g, 19.1 mmol) in dry THF (40 mL) was iodinated with NIS. Recrystallization from EtOAc afforded the desired iodide derivative **7** (3.94 g, 60%) in the form of small off-white needles. An analytical sample was prepared by dissolving the product in the minimum amount of boiling EtOAc, allowing the solution to cool to rt, and chilling the tightly-capped flask in a freezer overnight. M.p. 209–210 °C (dec); ^{1}H NMR (CD_3OD): $\delta = 2.44$ (s, 3H, CH_3), 5.29 (s, 2H, OCH_2Ph), 7.25–7.45 (m, 5H, Ar*H*); ^{13}C NMR ([D$_6$]DMSO): $\delta = 10.9$, 65.0, 86.2, 127.9, 128.0, 128.4, 130.5, 136.4, 139.6, 161.8; LRMS (CI+): m/z (%): 343 (100) $[M+H]^+$; HRMS (CI+): calcd for $C_{12}H_{12}N_2O_2I$ 342.9944; found 342.9934; elemental anaylsis calcd (%) for $C_{12}H_{11}N_2O_2$: C 42.13, H 3.42, N 8.19; found: C 42.27, H 3.34, N 8.01.

Diethyl 4,4′-dipropyl-2,2′-biimidazole-5,5′-dicarboxylate (8): A thick-walled pressure tube containing a stir bar was charged with iodide **5** (6.16 g, 20.0 mmol), $[Pd(PPh_3)_4]$ (0.92 g, 0.80 mmol), triethylamine[35] (4.05 g, 40.0 mmol), and dry toluene (30 mL). With stirring, a stream of argon was bubbled into the resulting gold-colored suspension for 10 min. The tube was sealed and heated to 110 °C for 48 h in the dark. During this time the reaction mixture became first homogeneous and dark brown. Then the crude product precipitated. The mixture was allowed to cool to ambient temperature and the crude product was collected by filtration. It was then washed with several 2 mL portions of ice-cold acetone until the washings were colorless. Recrystallization from methanol afforded **8** (1.01 g, 28%) in the form of fluffy white needles. M.p. 277–279 °C (dec); ^{1}H NMR ($CDCl_3$): $\delta = 0.85$ (t, 6H, $CH_2CH_2CH_3$), 1.19 (t, 6H, OCH_2CH_3), 1.62 (m, 4H, $CH_2CH_2CH_3$), 2.93 (t, 4H, $CH_2CH_2CH_3$), 4.25 (q, 4H, OCH_2CH_3); ^{13}C NMR ([D$_6$]DMSO): $\delta = 13.3$, 14.2, 22.4, 26.5, 59.1, 127.8, 137.3, 141.3, 162.8; UV/Vis (CH_2Cl_2): λ_{max} (ε M^{-1}cm^{-1}) = 294 (24000), 305 (22400), 318 (sh, 12300) nm; fluorescence emission (CH_2Cl_2): $\lambda_{max} = 352$ nm; LRMS (CI+): m/z (%): 363 (100) $[M+H]^+$, 725 (1) $[2M+H]^+$; LRMS (FAB+): m/z (%): 363 (62) $[M+H]^+$, 725 (1) $[2M+H]^+$; HRMS (CI+): calcd for $C_{18}H_{27}N_4O_4$ 363.2032; found 363.2031; elemental analysis calcd (%) for $C_{18}H_{26}N_4O_4$: C 59.65, H 7.23, N 15.46; found: C 59.55, H 7.18, N 15.36.

Diethyl 4,4′-dihexyl-2,2′-biimidazole-5,5′-dicarboxylate (9): A thick-walled pressure tube containing a stir bar was charged with the iodide derivative **6** (1.75 g, 5.00 mmol), $[Pd(PPh_3)_4]$ (0.23 g, 0.20 mmol), triethylamine (1.01 g, 10.0 mmol), and dry toluene (10 mL). With stirring, a stream of argon was bubbled into the gold-colored suspension for 10 min. The tube was sealed and heated to 110 °C for 48 h in the dark. A portion of the crude product precipitated upon cooling; it was collected by filtration, washed with small portions of ice-cold dichloromethane, and saved. The filtrate from this procedure was evaporated to a brown residue, and purified by flash column chromatography on silica gel using CH_2Cl_2/EtOAc (4:1 *v*/*v*) as the eluent. The fractions glowing blue under UV light were evaporated and combined with the crude product saved previously. Recrystallization from methanol afforded biimidazole **9** (0.49 g, 44%) as a white solid. M.p. 180–192 °C; t_R (CH_2Cl_2/EtOAc, 4:1): 0.35; ^{1}H NMR ($CDCl_3$): $\delta = 0.78$ (t, 6H, $CH_2CH_2CH_2CH_2CH_2CH_3$), 0.9–1.3 (br m, 18H, $CH_2CH_2CH_2CH_2CH_3$ and OCH_2CH_3), 1.51 (br m, 4H, $CH_2CH_2CH_2CH_2CH_3$), 2.89 (t, 4H, $CH_2CH_2CH_2CH_2CH_3$), 4.16 (q, 4H, OCH_2CH_3); ^{13}C NMR (CD_3OD): $\delta = 14.3$, 14.7, 23.6, 26.9, 30.0, 30.3, 32.7, 61.5, 129.3, 132.8, 138.8, 164.1; UV/Vis (CH_2Cl_2): λ_{max} (ε M^{-1}cm^{-1}) = 294 (24000), 306 (22100), 319 (sh, 11900) nm; fluorescence emission (CH_2Cl_2): $\lambda_{max} = 352$ nm; LRMS (CI+): m/z (%): 447 (100) $[M+H]^+$, 894 (39) $[2M+H]^+$, 1340 (11) $[3M+H]^+$, 1786 (1) $[4M+H]^+$; LRMS (FAB+): m/z (%): 447 (7) $[M+H]^+$, 893 (100) $[2M+H]^+$, 1340 (16) $[3M+H]^+$, 1786 (3) $[4M+H]^+$; HRMS (CI+): calcd for $C_{24}H_{38}N_4O_4$ 446.2893; found 446.2887; elemental analysis calcd (%) for $C_{24}H_{38}N_4O_4 \times 0.5(CH_3OH)$: C 63.61, H 8.72, N 12.11; found: C 63.65, H 8.57, N 12.24.

Dibenzyl 4,4′-dimethyl-2,2′-biimidazole-5,5′-dicarboxylate (10): A thick-walled pressure tube containing a stir bar was charged with iodide **7** (0.90 g, 2.6 mmol), $[Pd(PPh_3)_4]$ (0.12 g, 0.10 mmol), triethylamine (0.53 g, 5.2 mmol), and 20 mL of dry toluene. With stirring, a stream of argon was bubbled into the resulting gold-colored suspension for 10 min. The tube was sealed and heated to 110 °C for 48 h in the dark. Upon cooling to rt, the brown suspension was filtered through a sintered glass funnel. The

filter cake was washed with toluene (50 mL), and the filtrate was evaporated to dryness to yield a viscous, dark brown oil. This oil was purified by flash column chromatography on silica gel using CH_2Cl_2/EtOAc (2:1 *v*/*v*) as the eluent to afford **10** (0.22 g, 39%) as a light yellow solid. t_R (CH_2Cl_2/EtOAc 2:1): 0.38; ^{1}H NMR ($CDCl_3$): $\delta = 2.25$ (s, 6H, CH_3), 5.16 (s, 4H, OCH_2Ph), 7.10–7.25 (m, 10H, Ar*H*); ^{13}C NMR ($CDCl_3$): $\delta = 11.5$, 66.1, 128.2, 128.3, 128.5, 135.4, 137.2, 138.7, 162.7; UV/Vis (CH_2Cl_2): λ_{max} (ε $M^{-1}cm^{-1}$) = 293 (23000), 306 (21800), 320 (sh, 11700) nm; fluorescence emission (CH_2Cl_2): $\lambda_{max} = 354$ nm; LRMS (CI+): *m*/*z* (%): 431 (100) $[M+H]^+$, 861 (8) $[2M+H]^+$, 1291 (4) $[3M+H]^+$, 1721 (1) $[4M+H]^+$; LRMS (FAB+): *m*/*z* (%): 431 (85) $[M+H]^+$, 861 (6) $[2M+H]^+$, 1291 (1) $[4M+H]^+$; HRMS (CI+): calcd for $C_{24}H_{23}N_4O_4$ 431.1719; found 431.1706; elemental analysis calcd (%) for $C_{24}H_{22}N_4O_4 \times 0.5\,H_2O$: C 65.59, H 5.28, N 12.75; found: C 65.47, H 5.22, N 12.60.

Benzyl ethyl 4-methyl-4′-hexyl-2,2′-biimidazole-5,5′-dicarboxylate (11): A thick-walled pressure tube containing a stir bar was charged with iodide derivatives **6** (1.60 g, 4.56 mmol) and **7** (1.56 g, 4.56 mmol), $[Pd(PPh_3)_4]$ (0.42 g, 0.36 mmol), triethylamine (2.02 g, 20.0 mmol), and dry toluene (30 mL). With stirring, a stream of argon was bubbled into the resulting gold-colored suspension for 10 min. The tube was sealed and heated to 110 °C for 48 h in the dark. Upon cooling to rt, the brown suspension was filtered through a sintered glass funnel, and the filter cake was washed with toluene (50 mL). TLC analysis on silica plates of the filtrate using hexanes/EtOAc/CH_2Cl_2 (6:4:1 *v*/*v*/*v*) revealed the presence of three biimidazoles, **9** (fast spot), **10** (slow spot), and the desired **11** (middle spot). The filtrate was evaporated to dryness to yield a dark brown solid. This crude produce was subjected to flash column chromatography on silica gel using the eluent system described above. Recrystallization from methanol afforded **11** (0.29 g, 15%) as a cream-colored solid. M.p. 191–195 °C; t_R (hexanes/EtOAc/CH_2Cl_2 6:4:1): 0.20; ^{1}H NMR (CD_3OD): $\delta = 0.88$ (t, 3H, $CH_2CH_2CH_2CH_2CH_2CH_3$), 1.2–1.4 (br m, 6H, $CH_2CH_2CH_2CH_2CH_2CH_3$), 1.36 (t, 2H, OCH_2CH_3), 1.66 (br m, 2H, $CH_2CH_2CH_2CH_2CH_2CH_3$), 2.53 (s, 3H, CH_3), 2.95 (t, 2H, $CH_2CH_2CH_2CH_2CH_2CH_3$), 4.32 (q, 2H, OCH_2CH_3), 5.32 (s, 2H, OCH_2Ph), 7.3–7.5 (m, 5H, Ar*H*); ^{13}C NMR ([D_6]DMSO): $\delta =$ 11.0, 13.8, 14.2, 22.0, 24.8, 28.3, 29.1, 30.9, 59.3, 65.1, 117.8, 127.9, 128.0, 128.3, 128.5, 136.6, 137.2, 137.4, 137.5, 137.7, 137.8, 141.7, 141.9, 162.9, 163.0; UV/Vis (CH_2Cl_2): λ_{max} (ε $M^{-1}cm^{-1}$) = 294 (24100), 306 (22200), 320 (sh, 11700) nm; fluorescence emission (CH_2Cl_2): $\lambda_{max} = 354$ nm; LRMS (CI+): *m*/*z* (%): 439 (100) $[M+H]^+$, 878 (21) $[2M+H]^+$, 1316 (12) $[3M+H]^+$, 1755 (1) $[4M+H]^+$; LRMS (FAB+): *m*/*z* (%): 439 (100) $[M+H]^+$, 877 (18) $[2M+H]^+$, 1316 (2) $[3M+H]^+$; HRMS (CI+): calcd for $C_{24}H_{31}N_4O_4$ 439.2345; found 439.2326; elemental analysis calcd (%) for $C_{24}H_{30}N_4O_4$: C 65.74, H 6.90, N 12.78; found: C 65.48, H 6.88, N 12.64.

Dimethyl 4,4′-dipropyl-2,2′-biimidazole-5,5′-dicarboxylate (12): Biimidazole **8** (100 mg, 0.276 mmol) and sodium hydroxide (221 mg, 5.52 mmol) were combined in dry methanol (25 mL). The resulting mixture was heated to reflux under argon for 24 h. After cooling, the solvent was removed by using rotary evaporation, the residue was treated with dichloromethane (50 mL) and 1M aq HCl (50 mL), and the layers were separated. The aqueous layer was extracted with additional dichloromethane, and the combined organic phases were dried over Na_2SO_4. Filtration and evaporation of the filtrate gave a white solid, which was recrystallized from methanol to afford **12** (58 mg, 63%). M.p. 249–251 °C (dec); t_R (CH_2Cl_2/EtOAc 1:1): 0.35; ^{1}H NMR (CD_3OD): $\delta = 0.96$ (t, 6H, $CH_2CH_2CH_3$), 1.70 (m, 4H, $CH_2CH_2CH_3$), 2.95 (t, 4H, $CH_2CH_2CH_3$), 3.86 (s, 6H, OCH_3); ^{13}C NMR ([D_6]DMSO): $\delta = 13.3$, 22.3, 26.4, 50.5, 127.6, 137.3, 141.5, 163.3; UV/Vis (CH_2Cl_2): λ_{max} (ε $M^{-1}cm^{-1}$) = 293 (25000), 306 (22000), 320 (sh, 11000) nm; fluorescence emission (CH_2Cl_2): $\lambda_{max} = 348$ nm; LRMS (CI+): *m*/*z* (%): 335 (100) $[M+H]^+$, 669 (28) $[2M+H]^+$, 1003 (2) $[3M+H]^+$; LRMS (FAB+): *m*/*z* (%): 335 (100) $[M+H]^+$, 669 (2) $[2M+H]^+$; HRMS (CI+): calcd for $C_{16}H_{23}N_4O_4$ 335.1719; found 335.1719; elemental analysis calcd (%) for $C_{16}H_{22}N_4O_4$: C 57.47, H 6.63, N 16.76; found: C 57.32, H 6.77, N 16.61.

4,4′-Dimethyl-5,5′-dipropyl-2,2′-biimidazole (13): A stirred suspension of diester **8** (1.59 g, 4.39 mmol) in dry THF (40 mL) was cooled to 0 °C under argon. Lithium aluminum hydride (95%, 0.70 g, 18 mmol) was added in small portions over 3 min, during which time the mixture warmed and evolved H_2. The gray suspension was heated to reflux for 24 h. After cooling to rt, the mixture was carefully quenched by the dropwise addition of ice water until no more effervescence was observed. It was then filtered. The filter cake was washed with THF (300 mL), and the pink filtrate was diluted with EtOAc (300 mL). This organic solution was washed sequentially with 1M aq NaOH (100 mL) and brine, then dried over $MgSO_4$. Filtration and rotary evaporation of the filtrate provided the crude product as an off-white solid. This material was dissolved in the minimum amount of boiling EtOAc and the solution filtered while hot. After cooling to rt, the flask was chilled in a freezer overnight to give **13** (0.99 g, 92%) as off-white crystals. M.p. 206–208 °C (dec); t_R (CH_2Cl_2/CH_3OH 6:1): 0.73; ^{1}H NMR ($CDCl_3$): $\delta = 0.84$ (t, 6H, $CH_2CH_2CH_3$), 1.53 (m, 4H, $CH_2CH_2CH_3$), 2.12 (s, 6H, CH_3), 2.46 (t, 4H, $CH_2CH_2CH_3$); ^{13}C NMR (CD_3OD): $\delta = 10.7$, 13.9, 24.0, 28.2, 129.3, 133.2, 137.7; UV/Vis (CH_2Cl_2): λ_{max} (ε $M^{-1}cm^{-1}$) = 298 (18000), 305 (18700), 319 (sh, 11400) nm; fluorescence emission (CH_2Cl_2): $\lambda_{max} = 373$ nm; LRMS (CI+): *m*/*z* (%): 247 (100) $[M+H]^+$, 493 (12) $[2M+H]^+$, 732 (2) $[3M+H]^+$; LRMS (FAB+): *m*/*z* (%): 247 $[M+H]^+$, 493 (2) $[2M+H]^+$; HRMS (CI+): calcd for $C_{14}H_{23}N_4$ 247.1923; found 247.1919; elemental analysis calcd (%) for $C_{14}H_{22}N_4 \times \frac{1}{6}$EtOAc: C 67.49, H 9.01, N 21.46; found: C 67.35, H 8.90, N 21.48.

X-ray experimental for 12: Crystals grew as thin colorless needles by slow evaporation from a methanol solution. The data crystal was cut from a larger crystal and had approximate dimensions $0.19 \times 0.22 \times 0.56$ mm. The data were collected using the ω scan technique at 4–8° per min, with a scan range of 1.0° in ω to a $2\theta_{max} = 50°$ at 193 K on a Siemens P4 diffractometer, equipped with a Nicolet LT-2 low-temperature device and using a graphite monochromator with $Mo_{K\alpha}$ radiation ($\lambda = 0.71073$ Å). Details of crystal data, data collection, and structure refinement are listed in Table 1. The data were corrected for Lorentz polarization effects but not for absorption. The structure was solved by direct methods and refined by full-matrix least-squares on F^2 with anisotropic displacement parameters for the non-H atoms. The hydrogen atoms on carbon were calculated in ideal positions with isotropic displacement parameters set to 1.2 U_{eq} of the attached atom (1.5 U_{eq} for methyl hydrogen atoms). On molecule B, one propyl side chain was disordered about two orientations. The site occupancy was refined while refining a common isotropic displacement parameter for the atoms involved, C23B and C24B, and C23C and C24C. The site occupancy factor for C23B and C24B refined to 66(2)%. Thereafter, the displacement parameters were refined without constraint. The hydrogen atoms on the imidazole nitrogens were observed in a *F* map and refined with isotropic displacement parameters. One partial occupancy methanol molecule was located in the asymmetric unit. It was assigned a site occupancy factor of ½ after refining with unusually high U_{iso} values when the site occupancy factor was set to 1. Complete details are given in the Supporting Information.

X-ray experimental for 11: Crystals grew as colorless prisms by slow evaporation from methanol. The data crystal was cut from a larger crystal and had approximate dimensions $0.20 \times 0.30 \times 0.35$ mm. The data were collected on a Nonius Kappa CCD diffractometer using a graphite monochromator with $Mo_{K\alpha}$ radiation ($\lambda =$ 0.71073 Å). A total of 199 frames of data were collected using ω scans with a scan range of 1.9° and a counting time of 119 s per frame. The data were collected at −70 °C using a Oxford Cryostream low temperature device. Details of crystal data, data collection, and structure refinement are listed in Table 1. The structure was solved by direct methods and was refined in blocks by full-matrix least-squares on F^2 with anisotropic displacement parameters for the non-H atoms. The anisotropic displacement parameters were restrained during refinement to be approximately isotropic. The hydrogen atoms on carbon were calculated in ideal positions with isotropic displacement parameters set to 1.2 U_{eq} of the attached atom (1.5 U_{eq} for methyl hydrogen atoms). The hydrogen atoms on the imidazole nitrogen atoms were located from a ΔF map but were not subsequently refined. The positions were idealized with U_{iso} set to 1.2 U_{eq} of the bound nitrogen atom. There are six crystallographically independent molecules in the asymmetric unit. Due to the large number of atoms to be refined, the hexyl groups were restrained to have similar bond lengths and angles during refinement. Complete details are given in the Supporting Information.

X-ray experimental for 9: Crystals grew as thin colorless needles by slow cooling of a methanol solution. The data crystal was cut from a larger crystal and had approximate dimensions $0.14 \times 0.26 \times 0.76$ mm. The data were collected using the ω scan technique at 4–10° per min, with a scan range of 1.0° in ω to a $2\theta_{max} = 45°$ at 188 K on a Siemens P4 diffractometer, equipped with a Nicolet LT-2 low-temperature device and using a graphite monochromator with $Mo_{K\alpha}$ radiation ($\lambda = 0.71073$ Å). Details of crystal data, data collection, and structure refinement are listed in Table 1. The data were corrected for Lorentz polarization effects but not for absorption.

0947-6539/01/0703-0728 $ 17.50+.50/0 *Chem. Eur. J.* **2001**, *7*, No. 3

The structure was solved by direct methods and refined by full-matrix least-squares on F^2 with anisotropic displacement parameters for most of the non-H atoms. There are four molecules of the biimidazole and one-half molecule of methanol per asymmetric unit. The hydrogen atoms on carbon were calculated in ideal positions (C–H 0.96 Å) with isotropic displacement parameters set to 1.2 U_{eq} of the attached atom (1.5 U_{eq} for methyl hydrogen atoms). Several atoms of the hexyl groups and imidazole rings did not refine well (see the Supporting Information). The hydrogen atoms on the imidazole nitrogen atoms could not be found in a difference electron density map after all other atoms were accounted for, and were therefore not included in the final model. The site occupancy factors for the atoms of the methanol molecules were estimated to be 0.5 due to the amount of electron density in the region. Complete details are given in the Supporting Information.

Crystallographic data (excluding structure factors) for the structures reported in this paper have been deposited with the Cambridge Crystallographic Data Centre as supplementary publication no. CCDC-149173, -149174, and -149175. Copies of the data can be obtained free of charge on application to CCDC, 12 Union Road, Cambridge CB21EZ, UK (fax: (+44) 1223-336-033; e-mail: deposit@ccdc.cam.ac.uk).

Acknowledgement

W.E.A. was supported, in part, by an American Cancer Society Postdoctoral Fellowship. This work was further supported by grants from the National Science Foundation (CHE9725399) and the R.A. Welch Foundation (F-1018) to J.L.S.

[1] a) D. S. Lawrence, T. Jiang, M. Levett, *Chem. Rev.* **1995**, *95*, 2229–2260; b) D. B. Amabilino, J. F. Stoddart, *Chem. Rev.* **1995**, *95*, 2725–2828; c) A. E. Rowan, R. J. M. Nolte, *Angew. Chem.* **1998**, *110*, 65–71; *Angew. Chem. Int. Ed.* **1998**, *37*, 63–68; d) J.-M. Lehn, *Angew. Chem.* **1990**, *102*, 1347–1362; *Angew. Chem. Int. Ed. Engl.* **1990**, *29*, 1304–1319.

[2] a) G. R. Desiraju, *Science* **1997**, *278*, 404–405; b) S. C. Zimmerman, *Science* **1997**, *276*, 543–544; c) A. Gavezzotti, *Acc. Chem. Res.* **1994**, *27*, 309–314.

[3] M. C. Etter, *Acc. Chem. Res.* **1990**, *23*, 120–126.

[4] a) L. R. MacGillivray, J. L. Atwood, *Angew. Chem.* **1999**, *111*, 1080–1096; *Angew. Chem. Int. Ed.* **1999**, *38*, 1018–1033; b) J. J. Rebek, *Acc. Chem. Res.* **1999**, *32*, 278–286.

[5] J. S. Nowick, *Acc. Chem. Res.* **1999**, *32*, 287–296.

[6] B. Gong, Y.Yan, H. Zeng, E. Skrzypczak-Jankunn, Y. W. Kim, J. Zhu, H. Ickes, *J. Am. Chem. Soc.* **1999**, *121*, 5607–5608.

[7] A. P. Bisson, F. J. Carver, C. A. Hunter, J. P. Waltho, *J. Am. Chem. Soc.* **1994**, *116*, 10292–10293.

[8] R. E. Gillard, F. M. Raymo, J. F. Stoddart, *Chem. Eur. J.* **1997**, *3*, 1933–1940.

[9] S. C. Zimmerman, F. Zeng, D. E. C. Reichert, S. V. Kolotuchin, *Science* **1996**, *271*, 1095–1098.

[10] P. Lipkowski, A. Bielejewska, H. Kooijman, A. L. Spek, P. Timmerman, D. N. Reinhoudt, *Chem. Commun.* **1999**, 1311–1312.

[11] a) J.-M. Lehn, A. Marquis-Rigault, *Angew. Chem.* **1988**, *100*, 1121–1122; *Angew. Chem. Int. Ed. Engl.* **1988**, *27*, 1095–1096; b) D. M. Bassani, J.-M. Lehn, G. Baum, D. Fenske, *Angew. Chem.* **1997**, *109*, 1931–1933; *Angew. Chem. Int. Ed.* **1997**, *36*, 1845–1847.

[12] J. C. Nelson, J. G. Saven, J. S. Moore, P. G. Wolynes, *Science* **1997**, *277*, 1793–1796.

[13] G. S. Hanan, J.-M. Lehn, N. Krytsakas, J. Fisher, *Chem. Commun.* **1995**, 765–766.

[14] a) E. C. Constable, *Tetrahedron* **1992**, *48*, 10013–10059; b) E. C. Constable, F. Heirtzler, M. Neuburger, M. Zehnder, *J. Am. Chem. Soc.* **1997**, *119*, 5605–5617; c) E. C. Constable, M. Neuburger, L. A. Whall, M. Zehnder, *New J. Chem.* **1998**, 219–220; d) E. C. Constable, C. E. Housecroft, T. Kulke, G. Baum, D. Fenske, *Chem. Commun.* **1999**, 195–196.

[15] C. D. Eisenbach, U. S. Schubert, G. R. Baker, G. R. Newkome, *Chem. Commun.* **1995**, 69.

[16] J. D. Crane, J.-P. Sauvage, *New J. Chem.* **1992**, *16*, 649–650.

[17] a) S. Bhandari, C. G. Frost, C. E. Hague, M. F. Mahon, K. C. Molloy, *J. Chem. Soc. Dalton Trans.* **2000**, 663–669; b) D. L. Caulder, K. N. Raymond, *J. Chem. Soc. Dalton Trans.* **1999**, 1185–1200; c) M. J. Hannon, S. Bunce, A. J. Clarke, N. W. Alcock, *Angew. Chem.* **1999**, *111*, 1353–1355; *Angew. Chem. Int. Ed.* **1999**, *38*, 1277–1278; d) M. J. Hannon, C. L. Painting, N. W. Alcock, *Chem. Commun.* **1999**, 2023–2024; e) T. Imae, Y. Ikeda, M. Iida, N. Koine, S. Kaizaki, *Langmuir* **1998**, *14*, 5631–5635; f) C. Kaes, M. W. Hosseini, C. E. F. Rickard, B. W. Skelton, A. H. White, *Angew. Chem.* **1998**, *110*, 970–973; *Angew. Chem. Int. Ed.* **1998**, *37*, 920–922; g) J. J. Lessmann, W. D. J. Horrocks, *Inorg. Chem.* **2000**, *39*, 3114–3124; h) M. Munakata, L. P. Wu, T. Kuroda-Sowa, M. Maekawa, Y. Suenaga, G. L. Ning, T. Kojima, *J. Am. Chem. Soc.* **1998**, *120*, 8610–8618; i) G. W. Orr, L. J. Barbour, J. L. Atwood, *Science* **1999**, *285*, 1049–1052; j) H.-Y. Shen, D.-Z. Bu, Z.-H. Jiang, S.-P.;Yan, G.-L. Wang, *Inorg. Chem.* **2000**, *39*, 2239–2242; k) N.Yoshida, H. Oshio, T. Ito, *J. Chem. Soc. Perkin Trans. 2* **1999**, 975–983; l) M. Yamamoto, M. Takeuchi, S. Shinkai, *Tetrahedron Lett.* **2000**, *41*, 3137–3140; m) Y. Zhang, A. Thompson, S. J. Rettig, D. Dolphin, *J. Am. Chem. Soc.* **1998**, *120*, 13537–13538; o) D. Dolphin, A. Thompson, *J. Org. Chem.* **2000**, *65*, 7870–7877.

[18] a) S. J. Geib, C. Vincent, E. Fan, A. D. Hamilton, *Angew. Chem.* **1993**, *105*, 83–85; *Angew. Chem. Int. Ed. Engl.* **1993**, *32*, 119–121; b) T. Gulik-Krywicki, C. Fouquey, J.-M. Lehn, *Proc. Natl. Acad. Sci.* **1993**, *90*, 163–167; c) A. Singh, Y. Lvov, S. B. Qadri, *Chem. Mater.* **1999**, *11*, 3196–3200; d) L. J. Prins, J. Huskens, F. de Jong, P. Timmerman, D. N. Reinhoudt, *Nature* **1999**, *398*, 498–502; e) W. Yue, R. Bishop, M. L. Scudder, D. C. Craig, *Chem. Lett.* **1998**, 803–804; f) K. Tanaka, Y. Kitahara, *Chem. Commun.* **1998**, 1141–1142; g) M. Mazik, D. Bläser, R. Boese, *Tetrahedron Lett.* **1999**, *40*, 4783–4786; h) T. B. Norsten, R. McDonald, N. R. Branda, *Chem. Commun.* **1999**, 719–720; i) M. P. Lightfoot, F. S. Mair, R. G. Pritchard, J. E. Warren, *Chem. Commun.* **1999**, 1945–1946; j) J. H. K. K. Hirschberg, L. Brunsveld, A. Ramzi, J. A. J. M. Vekemans, R. P. Sijbesma, E. W. Meijer, *Nature* **2000**, *407*, 167–170; k) D. H. Appella, L. A. Christianson, D. A. Klein, D. R. Powell, X. Huang, J. J. J. Barchi, S. H. Gellman, *Nature* **1997**, *387*, 381–384.

[19] D. T. Cromer, R. R. Ryan, C. B. Storm, *Acta Crystallogr.* **1987**, *C43*, 1435–1437.

[20] B. H. Lipshutz, W. Vaccaro, B. Huff, *Tetrahedron Lett.* **1986**, *27*, 4095–4098.

[21] D. P. Mathews, J. P. Whitten, J. R. McCarthy, *J. Heterocycl. Chem.* **1987**, *24*, 689–692.

[22] D. P. Mathews, J. P. Whitten, J. R. McCarthy, *J. Org. Chem.* **1986**, *51*, 1891–1894.

[23] R. Kuhn, W. Blau, *Justus Liebigs Ann. Chem.* **1957**, *605*, 32–35.

[24] P. Schneiders, J. Heinze, H. Baumgärtel, *Chem. Ber.* **1973**, *106*, 2415–2417.

[25] K. Lehmstedt, H. Rolker, *Chem. Ber.* **1943**, *76*, 879–891.

[26] a) D. T. Cromer, C. B. Storm, *Acta Crystallogr.* **1990**, *C46*, 1957–1958; b) D. T. Cromer, C. B. Storm, *Acta Crystallogr.* **1990**, *C46*, 1959–1960.

[27] E. A. Falco, P. B. Russell, G. H. Hitchings, *J. Am. Chem. Soc.* **1951**, *73*, 3753–3758.

[28] R. Paul, J. A. Brockman, W. A. Hallett, J. W. Hanifin, M. E. Tarrant, L. W. Torley, F. M. Callahan, P. F. Fabio, B. D. Johnson, R. H. Lenhard, R. E. Schaub, A. Wissner, *J. Med. Chem.* **1985**, *28*, 1704–1716.

[29] M. R. Johnson, *J. Org. Chem.* **1997**, *62*, 1168–1172.

[30] M. D. Cliff, S. G. Pyne, *Synthesis* **1994**, 681–682.

[31] Details of the synthesis and characterization of 2-haloimidazoles which were not used in subsequent Pd^0-coupling reactions (i.e., **14**, **15**, and **16**) are given in the Supporting Information.

[32] For Ullmann coupling of 2-bromo-1-methyl-4,5-dicyanoimidazole, see: P. G. Apen, P. G. Rasmussen, *J. Am. Chem. Soc.* **1991**, *113*, 6178–6187.

[33] S. Knapp, J. Albaneze, H. J. Schugar, *J. Org. Chem.* **1993**, *58*, 997–998.

[34] M. Mammen, S.-K. Choi, G. M. Whitesides, *Angew. Chem.* **1998**, *110*, 2908–2953; *Angew. Chem. Int. Ed.* **1998**, *37*, 2754–2794.

[35] Preliminary experiments using *N*,*N*-diisopropylethylamine (40.0 mmol) instead of triethylamine in the coupling reaction increased the yield of **8** to 50–60%: H. Liu, M.Sc. Thesis, East Carolina University, **2000**.

Received: September 4, 2000 [F2710]